

Removal of reactive black 5 dye by using polyoxometalate-membrane

Ali Kemal Topaloğlu and Yilmaz Yildirim*

Department of Environmental Engineering, Zonguldak Bulent Ecevit University, Zonguldak, Turkey

(Received July 8, 2020, Revised January 28, 2021, Accepted February 1, 2021)

Abstract. A POM-membrane was fabricated by immobilizing a keggin type polyoxometalate (POM) $H_5PV_2Mo_{10}O_{40}$ onto the surface of microporous flat-sheet polymeric polyvinylidene fluoride (PVDF) membrane using a chemical deposition method. The POM-membrane was characterized by FT-IR, SEM and EDX to confirm existing of the POM onto the membrane surface. The POM-membrane was used to remove an anionic textile dye (Reactive Black 5 named as an RB5) from aqueous phases with a cross-flow membrane filtration and a batch adsorption system. The dye removal efficiency of the POM-membrane using the cross-flow membrane filtration system and the batch adsorption system was about 88% and 98%, respectively. The influence factors such as contact time, adsorbent dosage, pH, and initial dye concentration were investigated to understand the adsorption mechanism of the RB5 dye onto the POM-membrane. To find the best fitting isotherm model, Langmuir, Freundlich, BET and Harkins-Jura isotherm models were used to analyze the experimental data. The isotherm analysis showed that the Langmuir isotherm model was found to the best fit for the adsorption data ($R^2 = 0.9982$, $q_{max} = 24.87$ mg/g). Also, adsorption kinetic models showed the pseudo second order kinetic model was found the best model to fit the experimental data ($R^2 = 0.9989$, $q = 8.29$ mg/g, $C_0 = 15$ ppm). Moreover, after four times regeneration with HNO_3 acid, the POM-membrane showed high regenerability without losing dye adsorption capacity.

Keywords: polyoxometalates; membrane; adsorption; dye removal; reactive black

1. Introduction

Water pollution dramatically increased due to the most commonly used various toxic chemicals such as dyestuff, textiles, metals, paper, pharmaceuticals (Nesic *et al.* 2012, Vakili *et al.* 2016, Munagapati *et al.* 2018, Thirumoorthy and Krishna 2020). Among the various toxic pollutants, the dye wastewater resulting from the use of dyes have caused serious problems to against human health, biological organism, aquatic life and ecosystem (Heibati *et al.* 2014, Khan *et al.* 2018, Lafi *et al.* 2019). Reactive dyes such as RB5 have carcinogenic potentials and are difficult to natural degradability and the dyes can also be caused serious high pollutant load. Therefore, several methods such as membrane separation, biodegradation, chemical oxidation, flocculation, coagulation, adsorption, aerobic and anaerobic treatment are used for the removal of dye wastewater, but these removal methods for dye wastewater have some disadvantages (Ahmad *et al.* 2015, Khan *et al.* 2017, Lafi *et al.* 2019, Mahboub *et al.* 2020). In aerobic treatment, the dye color can be only removed at the end of the process due to the complex molecular structures of the dyes. In the anaerobic treatment of azo species, toxic and potentially carcinogenic aromatic amine compounds are formed (Laohaprapanon *et al.* 2015). The coagulation process provides effective color removal in insoluble dyes, but at

the same time, it is disadvantageous because of the cost of sludge (Yu *et al.* 2010). Similarly, the membrane systems such as nanofiltration (NF) and reverse osmosis (RO) require high pressure to treat dye wastewater although it has high removal efficiency without forming sludge. Also, the major disadvantage of these membrane systems is their high energy cost and low water permeability (Shao *et al.* 2013). In a new approach, catalytic oxidation may be used to treat dyes in wastewater for a short period but creating new problems in terms of recovery and reuse of the catalyst from the wastewater (Yao *et al.* 2016). Briefly, most of the methods have some advantages and disadvantages on their applications, but the adsorption process has some effective advantages such as no secondary pollution, low cost, its high removal efficiency in the dye removal from wastewater (Vakili *et al.* 2017, Munagapati *et al.* 2018). In the adsorption process, natural or synthetic products such as activated carbons, clays, chitosan beads, cellulose resin, polymeric resin, bottom ash were used as an adsorbent material (Ai *et al.* 2011, Ghaedi *et al.* 2014, Rache *et al.* 2014, Vakili *et al.* 2014, 2015, Li *et al.* 2017). In some studies, adsorption materials such as chitosan and clay have been added to membranes to produce adsorption membranes, combining adsorbent and membrane in one structure, and used to remove dyes and metals from aquatic environment and wastewaters (Wang *et al.* 2016, Li *et al.* 2017). In literature, the adsorption membranes achieved high removal efficiencies owing to their adsorption capabilities and membrane filtration properties in one structure. For example, Hebbar *et al.* (2018) fabricated an adsorptive membrane by modifying halloysite nanotubes

*Corresponding author, Ph.D., Professor
E-mail: yilmaz.yildirim@beun.edu.tr

(HNTs) into polyetherimide membrane matrix and the adsorption membrane showed rejection of 97% for methylene blue (MB) and 94% for Rhodamine B (Rh.B). It was also found the quantity of dye adsorbed (q_{max}) as 20.4 mg/g for MB and 19.6 mg/g for Rh.B in this study. In another study, Li *et al.* (2018) prepared chitosan nanofibrous membranes, and the adsorption capacity of the membrane was found as 1377 mg/g. These adsorption membranes show highly dye removal efficiency and have a high adsorption capacity.

In recent years, polyoxometalates (POMs) have been studied extensively on applications in a wide variety of fields such as catalysis, adsorption, medicine, and materials sciences (Muller *et al.* 1995, 2002, Ammam 2013). The POMs contain more than two metal atoms and usually have an anionic structure. The POMs are early transition metals having at least one shared oxygen atom in its structure (Ammam 2013). The POMs are high stability, low-cost, high performance and eco-friendly materials (Zhao *et al.* 2010, Putaj and Lefebvre 2011, Yao *et al.* 2013). A variety of studies has been conducted using the POMs for catalytic degradation of the macromolecules such as dyes and phenols in industrial wastewater. Apart from the catalytic properties of POMs, it has been revealed in some studies that it also has adsorption properties. For example, Rabbani *et al.* (2017) prepared heterometallic POM with keggings type ($Cs_4H_2PMo_{11}FeO_{40} \cdot 6H_2O$) as adsorbent and amount of adsorption (q_e) for methylene blue as cationic dye on the adsorbent was found 140.84 mg/g. In another study, Li *et al.* (2015) prepared $[Ni(bipy)_2]_2(HPW_{12}O_{40})$ as an adsorbent and amount of adsorption (q_e) for Rhodamine B dye as cationic dye on the adsorbent was found 22.75 mg/g. However, few studies on anionic dye removal using the POM-bound membrane are reported in the literature. $H_5PV_2Mo_{10}O_{40}$ as a POM has excellent adsorptive property on dye removal and these studies were carried out using the POM as an adsorbent. For example, Yao *et al.* (2014) prepared the POM incorporated membrane to remove 15 ppm RB5 as anionic dye wastewater by stirring (at 200 rpm) at 45°C, and the POM bound membrane showed excellent dye removal by adsorption process. It was found that dye removal efficiency was 97.5% at 120 min and the adsorption capacity of the membrane was 59.21 mg/g. It was also found that the POM bound membrane was excellent reusable without loss of dye removal efficiency in this study. In another study, Yao *et al.* (2016) using POM, fabricated the POM added membrane to remove 20 ppm RB5 as anionic dye wastewater by membrane filtration at 25°C and it was found 100% dye rejection owing to the adsorptive property of the POM. These studies have shown that the $H_5PV_2Mo_{10}O_{40}$ (POM) has high dye removal efficiency with its excellent adsorptive property of POM. However, in these studies, it has not been investigated the effects of various process parameters such as pH, contact time, initial dye concentration and has not also been studied the adsorption kinetic mechanism (pseudo first order, pseudo second order and intra-particle diffusion models) of the POM-bound membrane for anionic dyes.

According to the literature reviews conducted, since the studies on anionic dye removal using the POM-bound

membrane are few, this study attempted to fill the literature gaps in this subject. The aim of this study is to understand the removal and separation performance of the POM-membrane system and its adsorption mechanism. In this study, the POM-membrane was fabricated by modifying the laboratory-produced POM ($H_5PV_2Mo_{10}O_{40}$) onto the surface of the flat sheet PVDF membrane. The PVDF membrane was chosen owing to its high chemical resistance on the industrial wastewater treatment when compared with other polymeric membrane materials. Moreover, the PVDF membrane is cheaper and easier to produce than the ceramic membranes. When the membrane system is used with a module, it has more advantageous than the batch adsorption system. The removal and separation performance of the POM-membrane on the RB5 dye was evaluated using a cross-flow membrane filtration system. In the system, the experimental results showed that the dye removal was mainly achieved by adsorption process. After the adsorption process was determined to be dominant mechanism in the membrane filtration system, a batch system was used to eliminate the membrane filtration effect to fully reveal the adsorption mechanism. Therefore, main part of the present work was focused on adsorption process to evaluate the effect of adsorbent dosage, contact time, initial RB5 dye concentration, and pH on the removal performance of the POM-membrane. Additionally, the mechanism of the adsorption process was investigated using the adsorption isotherm models and kinetic models (pseudo-first order, pseudo-second order and intra-particle diffusion). The regenerability and reusability of the POM-membrane were also studied in the RB5 dye adsorption process.

2. Experimental

2.1 Materials

Commercial micro pores flat sheet membrane (average 0.2 µm pore diameter) was purchased from Microdyn-Nadir membranes, Germany. Sodium molybdate dehydrate ($Na_2MoO_4 \cdot 2H_2O$), concentrated sulphuric acid (H_2SO_4), disodium hydrogen phosphate (Na_2HPO_4), sodium metavanadate ($NaVO_3$), and diethyl ether were also purchased from Merck to synthesize 10-Molybdo-2-vanadophosphoric acid ($H_5PV_2Mo_{10}O_{40}$). 20 wt% poly diallyldimethylammonium chloride (PDDA), nitric acid (HNO_3) were purchased from Sigma-Aldrich. the RB5 dye was kindly supplied from DyStar. All chemicals purchased were analytical grade.

2.2 Synthesis of $H_5PV_2Mo_{10}O_{40}$

10-Molybdo-2-vanadophosphoric acid ($H_5PV_2Mo_{10}O_{40}$), a keggings-type polyoxometalate (POM), was synthesized according to the literature (Tsigdinos and Hallada 1968).

2.3 The POM-membrane fabrication

The commercial PVDF flat sheet membrane with an average of 0.2 µm pore diameter was used as a support

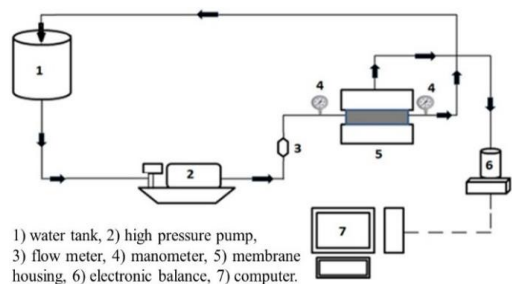


Fig. 1 Flow diagram of the cross-flow membrane system

layer for the POM loading. Firstly, the PVDF flat sheet membrane was submerged in an aqueous solution containing 1 wt% PDDA for 10 min and then dried at 40°C in a vacuum oven. Secondly, to immobilize the POM onto the PVDF membrane, the PVDF membrane was then submerged in an aqueous solution containing 1 wt% $PV_2Mo_{10}O_{40}^{-5}$ for 10 min and then dried at 40°C in the vacuum oven. The PVDF membrane modified with POM was formed and the membrane was washed by distilled water and finally dried in air to fabricate the POM-membrane. The details of the experimental study were given in the previous papers (Yao *et al.* 2013, Yıldırım and Topaloğlu 2018).

2.4 Characterization of the membranes

Unmodified PVDF membrane and the POM-membrane were characterized using Fourier transform infrared spektrofotometre (FT-IR), scanning electron microscopy (SEM) and energy dispersive X-ray (EDX). The membranes were characterized with a Perkin Elmer Pyris FT-IR at room temperature over a scanning range of 4000-600 cm^{-1} . scanning electron microscopy (SEM) measurements and energy dispersive X-ray (EDX) analysis of the membranes were performed by using the Zeiss EVO LS10 SEM coupled with the energy dispersive X-ray analyzer (SEM/EDAX). The unmodified PVDF membrane and the POM-membrane (at a voltage of 5 kV) were operated to analyze the surface morphology. The POM-membrane (at a voltage of 15 kV) were also operated to analyze the existence of relevant elements. The hydrophilic or hydrophobic properties of the unmodified PVDF membrane and the POM-membrane were investigated using the attension theta lite optical tensiometers. Also, pure water permeability (PWP) of the PVDF membrane and the POM-membrane were measured using the cross-flow membrane system having an effective surface area of $3 \times 5 cm^2$. Fig. 1 shows a schematic diagram of the cross-flow membrane filtration system. Pure water was circulated to measure the PWP at 1 bar transmembrane pressure (TMP). The permeability was measured using the computer-assisted system equipped with the AND EJ-6100 precision scales at certain time intervals. The PWP values were calculated using the following equation.

$$J_v = \frac{V}{S \times t} \quad (1)$$

where, J_v , V , S and t are defined as the permeation flux

$L/(m^2 \times h)$, the volume of the filtrate (liters), the effective membrane area (m^2) and the time (hour), respectively.

To explain the existence of RB5 dye onto the POM-membrane, thermogravimetry (TGA) analysis of membranes was performed using an SII Exstar TG/DTA 7200 from 30 to 900°C at 10°C/min in air atmosphere.

2.5 RB5 dye removal using microfiltration and batch systems

Membrane separation experiments were carried out using the cross-flow membrane filtration system (Fig. 1). A flat sheet membrane module (made from stainless steel) with a 15 cm^2 effective surface area ($3 \times 5 cm^2$) was used in the experiment. RB5 dye solution with 15 ppm concentration was filtered using the POM-membrane at 25°C and 0.5 bar (TMP). The residual dye concentration taken in the permeate site at certain times was determined by measuring at maximum wavelength of the RB5 ($\lambda_{max} = 597 nm$) using a UV-visible spectrophotometer (Shimadzu-1800). Also, batch experiments of RB5 dye removal by the POM-membrane were carried out in 100 ml of glass Erlenmeyer flask with a glass ground-in stopper and the solutions were shaken at 150 rpm in a shaker, at 25°C, and pH = 7. The POM-membrane as a fixed adsorbent (20 mg) was added into 10 ml of the RB5 dye solution (15 ppm). Control experiments (an unmodified PVDF membrane) were carried out under the same conditions. The residual dye concentration in the feed solution was determined by using a UV-visible spectrophotometer. For both experiments, the dye removal efficiency was calculated using the following equation.

$$\text{dye removal efficiency (\%)} = \frac{c_0 - c_t}{c_0} \times 100 \quad (2)$$

where, c_0 is initial dye concentration and c_t is the dye concentration at a certain time t of dye removal.

2.6 Batch adsorption studies of the RB5 dye

The RB5 dye was dissolved in distilled water to get a 100 mg/L stock solution. The POM-membrane as a fixed adsorbent (20 mg) was added into 10 ml of the RB5 dye solution with different concentrations (15, 30, 60 and 90 mg/L). Adsorption experiments were carried out in 100 ml of glass Erlenmeyer flask with glass ground-in stopper and the solutions were shaken at 150 rpm in a shaker, at 25°C, and pH = 7. The residual dye concentration in the solution was monitored and the capacity of adsorbed dye q_e (mg/g) was calculated using the following equation.

$$q_e = \frac{(c_0 - c_e)v}{m} \quad (3)$$

where, c_0 and c_e (mg/L) are the initial and equilibrium concentration of the RB5 dye solution, respectively. V (L) is the volume of working dye solution and m (g) is the weight of the used membrane.

2.7 Adsorption isotherm of the RB5 dye

It is important to investigate adsorption isotherm to find

out the relationship between the adsorbent and adsorbate. In literature, Langmuir and Freundlich isotherm models which are mostly applied but BET and Harkins-Jura isotherm models in the adsorption process were also used to investigate the adsorption performance of the POM-membrane for the RB5 dye in a batch system (Yao *et al.* 2014, Li *et al.* 2017, Munagapati *et al.* 2018). The Langmuir isotherm model describes that the adsorption of adsorbate is related to a homogenous surface of an adsorbent (Zheng *et al.* 2009, Thirumoorthy and Krishna 2020). It also assumes that the monolayer of adsorbate is covered on the surface of the adsorbent (Anbia *et al.* 2010, Patel and Hota 2014). The Langmuir isotherm is given by the following equation.

$$\frac{c_e}{q_e} = \frac{1}{k_L q_{max}} + \frac{c_e}{q_{max}} \quad (4)$$

where q_{max} is maximum adsorption capacity (mg/g) and k_L (L/mg) is rate of adsorption.

The important characteristic of the Langmuir isotherm can be explained in terms of a dimensionless equilibrium parameter (R_L) and the parameter is calculated using the Eq. (5).

$$R_L = \frac{1}{(1 + k_L c_0)} \quad (5)$$

The Freundlich isotherm model describes that the adsorption of adsorbate is related to a heterogeneous surface of an adsorbent. It also assumes that the multilayer of adsorbate is covered on the surface of the adsorbent (Anbia *et al.* 2010, Patel and Hota 2014). The Freundlich isotherm is given in Eq. (6).

$$\log q_e = \log k_F + \frac{1}{n} \log c_e \quad (6)$$

where k_F is the adsorption capacity (mg/g) and $1/n$ is the adsorption intensity.

The BET isotherm model is given in Eq. (7) (Arami *et al.* 2006).

$$\frac{c_e}{(c_s - c_e)q_e} = \frac{1}{k_b q_m} + \frac{k_b - 1}{k_b q_m} \times \frac{c_e}{c_0} \quad (7)$$

where q_m , k_b and c_s are amount of dye solution adsorbed when forming a complete monolayer (mg/g), a constant of the BET isotherm model and saturation concentration of dye solute (mg/L), respectively.

The Harkins-Jura isotherm model is given in Eq. (8) (Liu and Wang 2013).

$$\frac{1}{q_e^2} = \frac{B_{HJ}}{A_{HJ}} - \frac{1}{A_{HJ}} \log c_e \quad (8)$$

where A_{HJ} and B_{HJ} are constants on the Harkins-Jura isotherm model.

2.8 Adsorption kinetics of the RB5 dye

Kinetic experiments were carried out to determine the contact time needed to reach equilibrium and adsorption rates of the dye. In the kinetic experiments, 20 mg of the POM-membrane was put into 10 ml of dye solutions using

four different dye concentrations (15, 30, 60 and 90 mg/L). The mixture was shaken at 150 rpm, 25°C, and pH = 7. Samples from dye solutions were taken at certain times intervals during the experiment and residual dye concentration of the samples were determined by UV-vis spectroscopy. The capacity of adsorbed dye q_t (mg/g) was calculated according to the following equation.

$$q_t = \frac{(c_0 - c_t)v}{m} \quad (9)$$

where q_t (mg/g) is adsorption capacity and c_t (mg/L) is the concentration of the RB5 dye at a certain time t of the dye solution.

The obtained data were used to explain the adsorption mechanism of the RB5 dye on the POM-membrane employing two kinetic models (pseudo first-order and pseudo second-order). The pseudo first-order kinetic model shows that the rate of change of surface site concentration is proportional to the amount of remaining uncopied surface sites (Nesic *et al.* 2012). The pseudo first-order kinetic model equation is given in Eq. (10).

$$\log(q_e - q_t) = \log q_e - \frac{k_1 t}{2.303} \quad (10)$$

where, q_t (mg/g) is the adsorption capacity of the POM-membrane at the time (minute), k_1 (min^{-1}) is the adsorption rate constant of pseudo first order kinetic model.

Values of q_e and k_1 can be calculated from the intercept and slope of the plot of $\log(q_e - q_t)$ versus t , respectively. The pseudo second order kinetic model shows that the rate is proportional to the square of the number of remaining free surface sites (Nesic *et al.* 2012). The pseudo second-order kinetic model equation is given in Eq. (11).

$$\frac{t}{q_t} = \frac{1}{k_2 q_e^2} + \frac{t}{q_e} \quad (11)$$

where, k_2 (g/mg/min) is the adsorption rate constant of pseudo second order kinetic model. Values of q_e and k_2 can be determined from the intercept and slope of plots of t/q_t versus t , respectively.

2.9 Intra-particle diffusion model

The pseudo first order and pseudo second order kinetic models cannot describe the diffusion mechanism (Nesic *et al.* 2012). Therefore, in this study, the intra-particle diffusion model was used to describe the diffusion mechanism of the RB5 dye on the POM-membrane and to estimate the rate-limiting step in the porous structure. The diffusion model was developed by Weber and Morris to describe the diffusion mechanism (Weber and Morris 1963, Nesic *et al.* 2012). The intra-particle diffusion model equation is given in Eq. (12).

$$q_t = k_{id} t^{1/2} + c \quad (12)$$

where q_t (mg/g) is the adsorption capacity of time, $t^{1/2}$ ($\text{min}^{1/2}$) is the square of the time, the k_{id} (mg/(g.min^{1/2})) is the intra-particle diffusion rate constant, c (mg/g) is a constant that gives the effect of bounding layer on molecule diffusion. Values of k_{id} and c can be found from the slope and intercept of plots of q_t versus $t^{1/2}$, respectively.

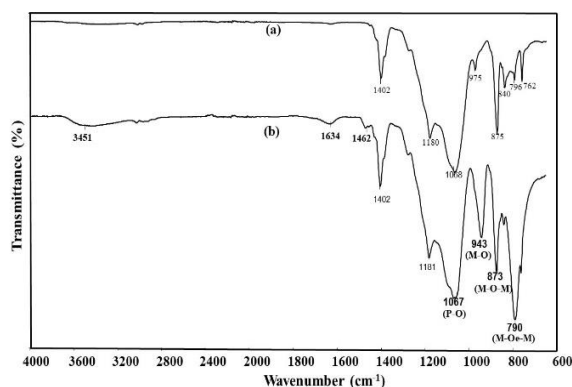
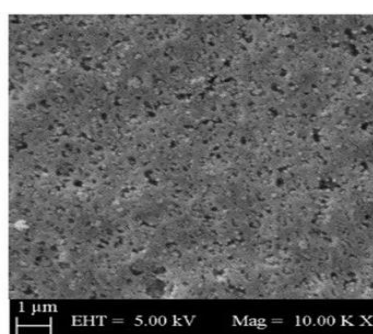
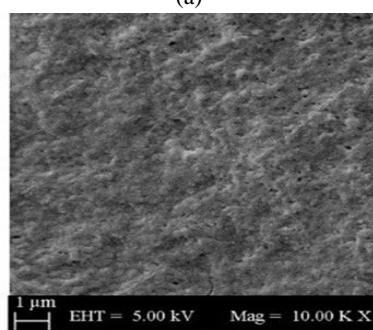


Fig. 2 FT-IR spectra of (a) the unmodified membrane; (b) the POM-membrane. M; Mo or V, Oe; edge-sharing oxygen, Oc; corner-sharing oxygen



(a)



(b)

Fig. 3 SEM images of the membrane surface (a) the unmodified membrane; (b) the POM-membrane

2.10 Reuse of the POM-membrane

To regenerate, the POM-membrane was taken out from the RB5 dye solution and immersed in 50% HNO₃ solution to remove the adsorbed dye, and followed by washing with distilled water until the neutral pH was obtained. After regeneration, the POM-membrane was used for adsorption again to investigate the influence of recycling times on the adsorption capacity of the POM-membranes.

3. Results and discussion

3.1 Characterization of membranes

In the FT-IR analysis, the unmodified membrane and the

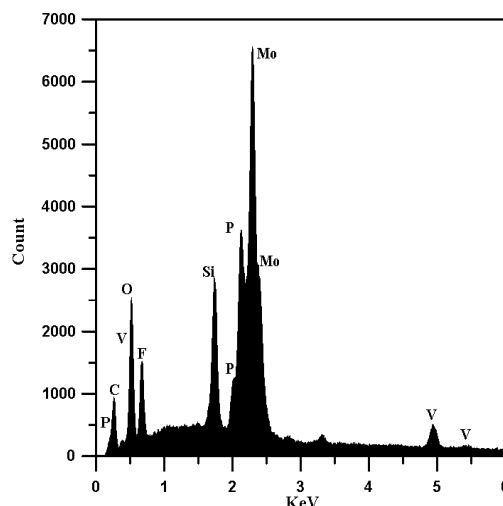


Fig. 4 EDX spectrum of the POM-membrane

POM-membrane were analyzed. Figs. 2(a) and (b) show the bands of the unmodified PVDF membrane and the PVDF membrane modified with POM (POM-membrane). The POM-membrane has four characteristic peaks of the POM. Two of the peaks 943 cm⁻¹ v(M-O) and 790 cm⁻¹ v(M-Oe-M) showed very sharp and dense peaks. Similar results were observed in the literature (Tangestaninejad *et al.* 2010, Yao *et al.* 2013). Furthermore, as seen in Fig. 2(b), the two general bands of the Keggin-type polyoxometalate, P-O, and M-Oc-M bands have existed at 1067 and 873 cm⁻¹ (Kumar and Landry 2007, Yao *et al.* 2013). The characterized bands of the PDDA (Zhang *et al.* 2011, Yao *et al.* 2013) were observed at 3451 cm⁻¹, 1634 cm⁻¹ and 1462 cm⁻¹ (Fig. 2(b)), confirming the existence of the PDDA on the membrane. The details of the study can be found in the previous study (Yıldırım and Topaloğlu 2018).

The surface morphologies of the unmodified membrane and the POM-membrane were analyzed by SEM (Figs. 3(a) and (b)). The unmodified membrane and the POM-membrane have a micro-porous structure (Figs. 3(a) and (b)). The pore sizes of the POM-membrane were slightly narrowed after the modification of the membrane by the POM (Fig. 3(b)).

By EDX, the POM-membrane was analyzed. Fig. 4 shows that the POM-membrane consists of V, O, P, and Mo elements belonging to the POM. C and F elements in the POM-membrane were due to the existence in the structure of the PVDF membrane. As a result, the POM-membrane was successfully fabricated according to EDX analysis. The details of the study can be found in a previous study (Yıldırım and Topaloğlu 2018).

The contact angles of the unmodified membrane and the POM-membrane were measured. It was found that the contact angle of the unmodified membrane was 78.78° and that of the POM-membrane was 54.11°. According to these results, the hydrophilicity of the POM-membrane increased. This is because the POM is a hydrophilic material and it increases the hydrophilicity as indicated in the literature (Yao *et al.* 2013).

The pure water permeability (PWP) value of the PVDF membrane (before the modification) and the POM-

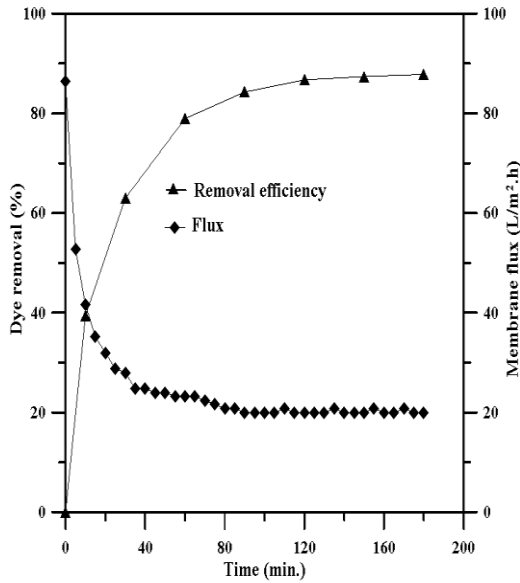


Fig. 5 RB5 dye removal using the POM-membrane (15 cm² POM-membrane, 15 ppm RB5 (6L), 25°C, pH = 7)

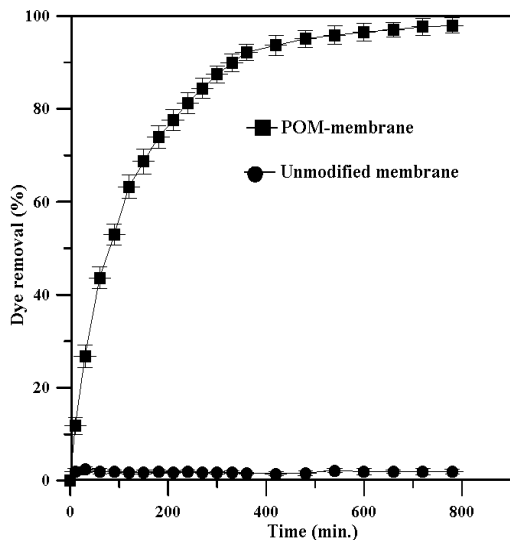


Fig. 6 RB5 dye removal using the POM-membrane and the unmodified membrane (20 mg membrane weight), 15 ppm RB5 (10 ml) dye, T = 25°C, 150 rpm, pH = 7)

membrane (after modification of the PVDF membrane with POM) were measured as 1038 ± 68 L/m².h.bar and 128 ± 4 L/m².h.bar, respectively. The PWP value of POM-membrane fabricated after modification of the PVDF membrane with POM was still in the range of the microfiltration membrane.

3.2 Dye removal test

Fig. 5 shows the dye removal efficiency of the POM-membrane. In the permeate site, the removal efficiency was quickly increased up to 75% within the 50 min and then reached a stable level (88%) in the 100 min. Similarly, the flux value of POM-membrane decreased quickly from 86.4 L/m².h to 24 L/m².h in the first 50 min and then reached a stable level of about 20 L/m².h in the 100 min (Fig. 5). It

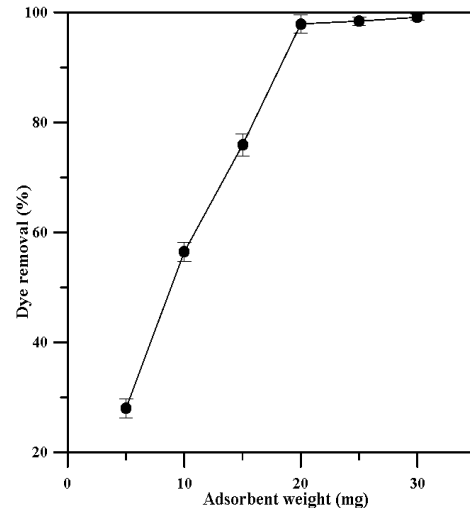


Fig. 7 Effect of adsorbent dosage on removal of RB5 dye at a fixed condition with dye concentration (15 mg/L), pH = 7, T = 25°C and contact time = 780 min

may be explained that the reason for the rapid decline in the flux and the rapid increase in dye removal efficiency was due to the adsorption of dye by the POM-membrane (Sahoo *et al.* 2016, Zhang *et al.* 2020). To eliminate the influence of the membrane filtration, only the batch system was used to investigate the adsorption effect of the POM-membrane in the next experiments.

In the batch system, the POM-membrane and the unmodified membrane (contrast sample) were used to evaluate the dye removal efficiency of the POM-membrane by contrast experiments. Equal membrane weight of 20 mg was put into 2 portions of RB5 dye aqueous solution (15 ppm, 10 ml) with shaking at 150 rpm in a shaker, at 25°C and pH = 7. Fig. 6 shows that the POM-membrane exhibited the very high dye removal efficiency toward the RB5 dye. About 90% dye removal efficiency was achieved in 300 min and about 98% dye removal efficiency reached in the testing period 780 min. Whereas, the unmodified membrane (as a control sample) exhibited very low dye removal efficiency. So, the adsorption capacity of the unmodified membrane toward the dye can be ignored. A similar result was found by Yao *et al.* (2014) using the SEP-M membrane as a polyoxometalate material to treat the RB5 dye by adsorption process, providing 97.5% dye removal efficiency at 200 rpm and 45°C.

3.3 Adsorption studies

3.3.1 Effect of adsorbent dosage

The effect of the POM-membrane dosages on the removal of RB5 dye was investigated using 5-30 mg of the adsorbent. As seen in Fig. 7, when the POM-membrane dosage increased from 5 to 20 mg, the percentage of the RB5 dye removal increased very fast and then reached its removal value of about 98% at 20 mg of the adsorbent dosage. This result may be explained as a result of the increase in the more vacant active sites of the adsorbent with increasing adsorbent dosage (Li *et al.* 2017, Thirumorthy and Krishna 2020). However, the percentage

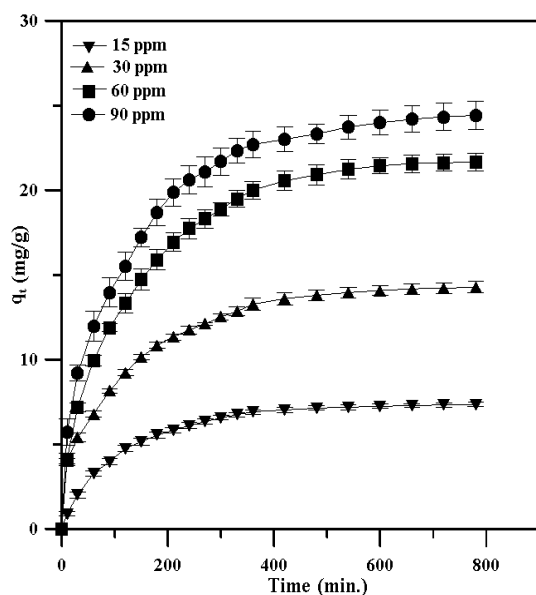


Fig. 8 The equilibrium adsorption capacity of different RB5 dye concentration as a function of time ($T = 25^{\circ}\text{C}$, $\text{pH} = 7$ at 150 rpm)

of the RB5 dye removal remained almost unchanged level when more than 20 mg of the dosage was used. Therefore, the optimum adsorbent dosage for the RB5 dye was selected as 20 mg.

3.3.2 Effect of contact time and initial concentration

Determining the equilibrium time in the adsorption process is greatly important in terms of the economical design of wastewater treatment systems (Özer and Dursun 2007, Güzel *et al.* 2015). Fig. 8 shows the contact time effect and initial dye concentration effect on the adsorption of the RB5 dye on the POM-membrane. The adsorption amount of RB5 dye increased rapidly until the contact time reached about 400 minutes. Then the adsorption amount of RB5 dye decreased gradually and reached equilibrium. It can be explained that the reason of the fast adsorption of the RB5 dye at the beginning stage, all active surface of the adsorbent was available due to the existence of many vacant adsorption sites but after this fast adsorption, slow adsorption occurred due to decreasing in vacant adsorption sites (Güzel *et al.* 2015, Rajabi *et al.* 2015, Li *et al.* 2017, Thirumorthy and Krishna 2020). Also, the saturated adsorption amount reached from 7.34 to 24.42 mg/g as the initial RB5 dye concentration was increased from 15 to 90 mg/L (Fig. 8). Similar results were recorded on many studies in the literature (Roesink *et al.* 1991, Güzel *et al.* 2015, Ben-Ali *et al.* 2017, Wong *et al.* 2019, Zhang *et al.* 2020). The reason for the increase of the adsorption capacity with the increasing initial RB5 dye concentration may be explained by a driving force for adsorption of the RB5 dye towards the surface of the POM-membrane (Baral *et al.* 2009, Hebbbar *et al.* 2018, Zhang *et al.* 2020). However, when the RB5 dye concentration was increased above 60 mg/L, the adsorption amount of dye slowly increased, indicating that sites of the adsorbent reached its saturation level.

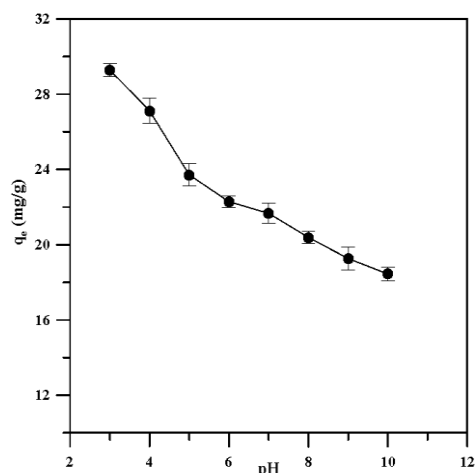


Fig. 9 pH effect of the adsorption capacity of RB5 dye (60 ppm) on the POM-membrane ($T = 25^{\circ}\text{C}$ at 150 rpm)

3.3.3 Effect of pH

The effect of solution pH is one of the most important roles for the adsorption process. It controls the ionization degree of different functional groups of the adsorbate, the surface charge of the adsorbent and the adsorption mechanism (Munagapati *et al.* 2018, Thirumorthy and Krishna 2020). The effect of solution pH was studied under the conditions of the RB5 dye concentration (60 mg/L), the POM-membrane weight (20 mg) as an adsorbent, by shaking (at 150 rpm) and contact time (780 min.). Fig. 9 shows that adsorption capacity decreased as pH level increased from 3 to 10 and maximum adsorption capacity (29.28 mg/g) was observed at pH 3.0. The adsorption capacity for ionic dye under lower pH (acidic environment) is bigger than that of higher pH (alkaline environment). It can be explained that under lower pH, as the concentration of H^+ ions on the surface of adsorbent increases, a positively charged on the surface of adsorbent increases, resulting in the electrostatic attraction between positively charged surface of the adsorbent and anionic dye molecules. However, under higher pH, as the OH^- ion concentration on the surface of the adsorbent increase, a negatively charged on the surface of the adsorbent increase, leading to electrostatic repulsion between the negatively charged surface of the adsorbent and anionic dye molecules. As a result, when the pH of the solution became acidic, the maximum adsorption capacity of the RB5 dye on the POM-membrane increased due to the increasing electrostatic attraction force. In a lot of research, it was reported that adsorption for anionic dye under a lower pH (acidic environment) was more effective (Yang *et al.* 2011, Güzel *et al.* 2015, Munagapati *et al.* 2018).

3.4 Adsorption isotherms

The adsorption isotherm models were used to evaluate the interactions between the RB5 dye and the POM-membrane. Fig. 10 shows the effect of the initial RB5 dye concentration on the adsorption capacity of the POM-membrane. As initial dye concentration was increased, the adsorption capacity of the POM-membrane increased. The

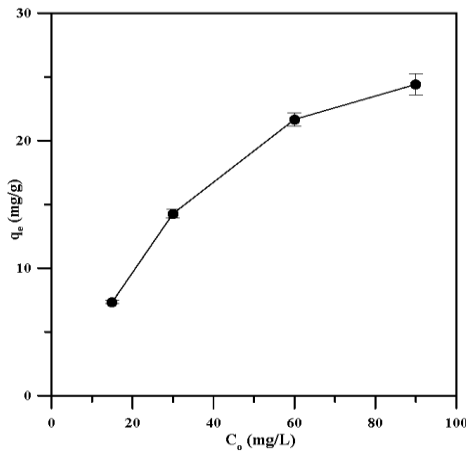


Fig. 10 Effect of the RB5 dye initial concentration (15, 30, 60 and 90 mg/L) on the adsorption capacity of the POM-membrane (T = 25°C, pH = 7 at 150 rpm)

POM-membrane reached maximal adsorption capacity 24.42 mg/g under the initial RB5 concentration of 90 mg/L. Also, the adsorbed amount reached an almost stable level at the RB5 dye concentration of 90 mg/L.

Langmuir, Freundlich, BET and Harkins-Jura isotherm models were applied to investigate the surface properties and affinity of the RB5 dye onto the POM-membrane. The adsorption was found to fit better the Langmuir isotherm model. This is because the correlation coefficient (R^2) for the Langmuir isotherm model was much bigger than that for the Freundlich isotherm model as seen in Table 1. Also, the theoretical maximum adsorption capacity of the POM-membrane for the Langmuir isotherm model was calculated as 24.87 mg/g and the value was observed to be mostly close to the experimental maximum adsorption capacity of the POM-membrane (24.42 mg/g). According to these results, the adsorption site of the POM-membrane was homogenous and the monolayer of RB5 dye was covered on the surface of the adsorbent. (Li *et al.* 2018).

The R_L is used to find the adsorption efficiency of the

Table 1 Result of the isotherm models for the adsorption of RB5 dye

Langmuir isotherm model			
q_{max} (mg/g)	K_L (L/mg)	R^2	R_L
24.87	0.782	0.9982	(0.014-0.078)
Freundlich isotherm model			
K_F (mg/g)	1/n	R^2	
10.944	0.235	0.9390	
BET isotherm model			
q_m (mg/g)	K_b	R^2	
13.86	240.33	0.9859	
Harkins-Jura			
A_{HJ}	B_{HJ}	R^2	
138.89	1.56	0.7653	

adsorption process. If R_L value is between 0 and 1, it illustrates favorable adsorption, but if it is bigger than 1, it illustrates unfavorable adsorption. As seen in Table 1, the R_L values for RB5 dye concentrations (15-90 ppm) were found to be in the range of 0.014-0.078, illustrating the favorable adsorption processes of the RB5 dye onto the POM-membrane. Also, for the Freundlich isotherm model if the value of 1/n is larger than 2, it means poor adsorption, but if the value of 1/n is between 0.1 and 0.5, it means that the adsorbent is easily adsorbed (Xiong *et al.* 2016, Zhang *et al.* 2020). In this study, the value of 1/n was calculated as 0.235, and therefore it can be expressed that RB5 dye was easily adsorbed on the POM-membrane.

3.5 Adsorption kinetics

The adsorption kinetics was studied using the different initial concentrations of the RB5 dye. For initial the RB5 dye concentrations of 15, 30, 60 and 90 mg/L, the adsorption equilibrium amounts were experimentally found

Table 2 Kinetik constant of RB5 dye adsorption onto the POM-membrane (T = 25°C, pH = 7 at 150 rpm)

	c_0 (mg/L)	15	30	60	90
Pseudo-first order model	q_e (mg/g) (experimental)	7.34	14.27	21.66	24.42
	q_1 (mg/g)	7.01	12.79	23.19	21.01
	k_1 (10^{-3} L/min)	7.599	7.139	7.830	6.909
	R^2	0.9938	0.9917	0.9791	0.9836
Pseudo-second order model	q_2 (mg/g)	8.29	15.6	24.15	26.67
	k_2 (10^{-3} g/(mg min))	1.39	0.91	0.5	0.54
	R^2	0.9989	0.9973	0.9977	0.9981
Intra-particle diffusion model	k_{id1} (mg/(g \times min $^{-1/2}$))	0.3755	0.5948	0.9947	1.0756
	c_1 (mg/g)	0.2068	2.3986	1.9915	3.446
	R^2	0.9744	0.9888	0.9874	0.9848
	k_{id2} (mg/(g \times min $^{-1/2}$))	0.0417	0.09	0.15	0.1957
	c_2	6.2017	11.82	17.65	19.09
	R^2	0.9692	0.9587	0.9161	0.968

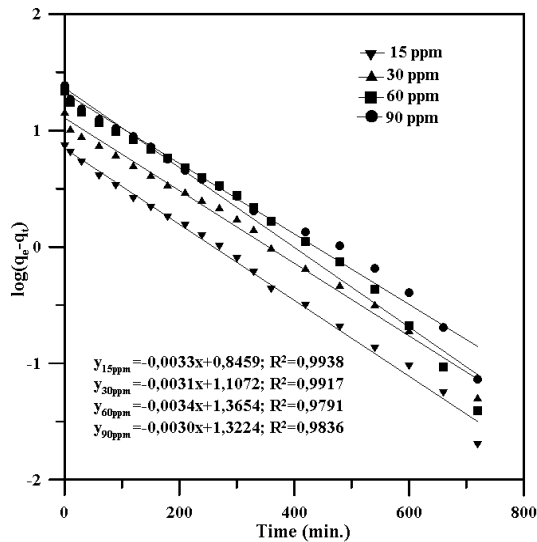


Fig. 11 Pseudo first order for the RB5 dye adsorption onto the POM-membrane ($T = 25^\circ\text{C}$, $\text{pH} = 7$ at 150 rpm)

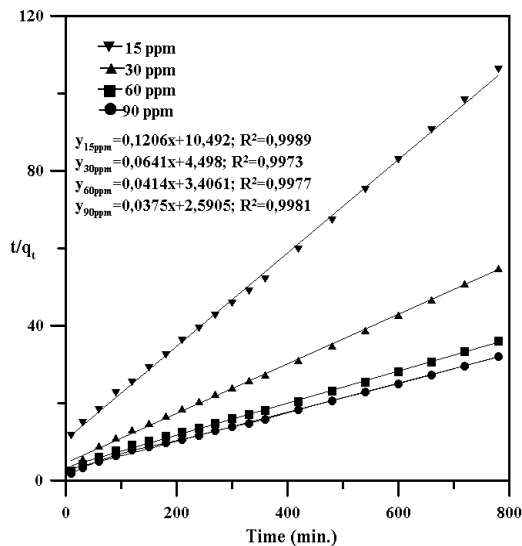


Fig. 12 Pseudo second order for the RB5 dye adsorption onto the POM-membrane ($T = 25^\circ\text{C}$, $\text{pH} = 7$ at 150 rpm)

as 7.34, 14.27, 21.66 and 24.42 mg/L, respectively (Table 2). To investigate the adsorption process of the RB5 dye onto the POM-membrane, pseudo first order kinetics (Fig. 11) and pseudo second order kinetics (Fig. 12) were employed to relate experimental data. Table 2 showed that pseudo second order kinetic model provided a better fit than pseudo first order kinetic model according to correlation coefficients (R^2). Moreover, q_e values found for the pseudo second order kinetic model were determined to be much closer to the q_e values found by the experimental measurement than those for the pseudo first order kinetic model as given in Table 2. Consequently, it was found that the pseudo second order kinetic model was a better fit to describe the adsorption onto the POM-membrane.

3.6 Intra-particle diffusion model

Fig. 13 shows intra-particle diffusion plots of the

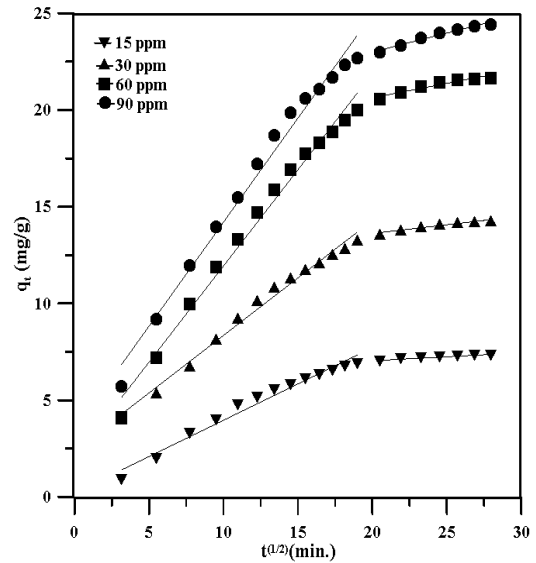


Fig. 13 Intra particle diffusion model of the RB5 dye adsorption onto the POM-membrane ($T = 25^\circ\text{C}$, $\text{pH} = 7$ at 150 rpm)

different initial RB5 dye concentration onto the POM-membrane. The plots were not linear during the whole time and did not pass over the origin (Fig. 13). Also, the R^2 values of the intra-particle diffusion model (0.9161-0.9888) were found to be lower than that of the pseudo second order kinetic model (0.9973-0.9989). Therefore, it can be explained that the intra-particle diffusion was not the only rate-limiting step. The result showed the adsorption mechanism of RB5 dye onto the POM-membrane is complex and involves another mechanism as indicated in the literature (Du *et al.* 2014, Li *et al.* 2017). The k_{id1} and k_{id2} constant values increased as the RB5 dye concentrations increased from 15 to 90 mg/L (Table 2). It can be explained that the adsorption driving force and the adsorption of the RB5 dye molecules onto the surface of the POM-membrane caused to increase when working under the high RB5 dye concentration. Similar results were reported for the adsorption process previously by other studies (Ahmed *et al.* 2017, Zhang *et al.* 2020).

3.7 Regeneration capacity of the POM-membrane

The regeneration property shows the stability of the adsorbent. It is assumed that even after several regenerations, the reusability of the adsorbent is an important criterion for practical applications (Xin *et al.* 2017, Li *et al.* 2018). In this study, the used membranes after the dye adsorption experiment were regenerated firstly by HNO_3 solution for 5 min and then washed with distilled water. After the regeneration, the regenerated membrane was used repeatedly four times to evaluate the reusable properties of the membranes in the processes of the adsorption-desorption cycle, and the equilibrium adsorption capacities of the membranes were shown in Fig. 14. After the five adsorption experiment, the equilibrium adsorption capacity still reached 6.85 mg/g and the relative ratio of the adsorption capacity calculated by $q_{e,5}/q_{e,1}$ was about 93%

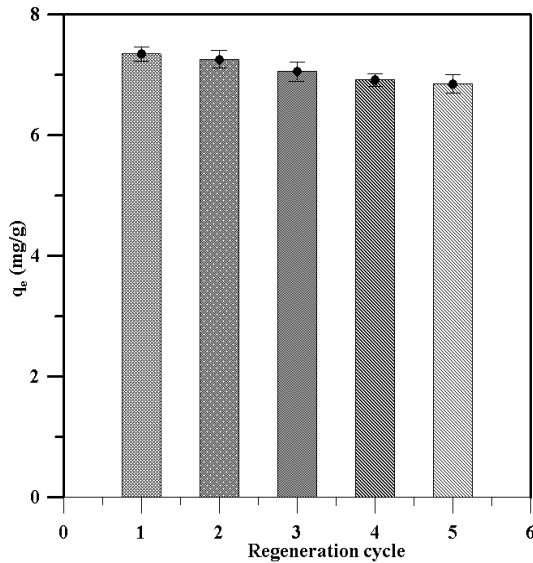


Fig. 14 Five consecutive regeneration cycles of the POM-membrane for the adsorption of RB5 dye (RB5 = 15 mg/L, T = 25°C, pH = 7 at 150 rpm)

($q_{e,5}$, $q_{e,1}$ were the final adsorption cycle value and the first adsorption cycle value). These results may be explained that vacant adsorption sites of adsorbent were slightly missed or weakened during the regeneration process using HNO_3 solution and then distilled water (Hosseini *et al.* 2016, Li *et al.* 2018). Also, these results show high regenerable and reusable of the POM-membrane in the RB5 dye removal.

4. TGA analysis of the POM-membrane before and after dye adsorption

To prove acting as an adsorption membrane of the POM-membrane, TGA analysis was conducted to figure out any weight losses before and after the RB5 dye removal studies of the POM-membrane. Considering ‘curve a’ in Fig. 15, the highest level of weight loss appeared at 300-445°C for the POM-membrane before the RB5 dye removal studies, which is related to the decomposition of the POM and PVDF. Concerning ‘curve b’ in Fig. 15, the highest level of weight loss appeared at 400-485°C for the POM-membrane after the RB5 dye removal studies. After dye removal by the POM-membrane, it can be obviously seen to be different from the original one, displaying the existence of the RB5 dye onto the POM-membrane. On the other hand, it has appeared that a membrane encapsulated POM showed a similar adsorption effect of the RB5 dye in the literature (Yao *et al.* 2014). Also, the adsorption of the RB5 on the POM-membrane has a complicated mechanism and can be attributed to various interactions such as hydrogen bonding, hydrophobic interaction and electrostatic interaction (Wang *et al.* 2014, Yao *et al.* 2016). Since the POM-membrane includes the PDDA polymer containing cationic amino groups, it is assumed that the electrostatic interaction might have occurred between the POM-membrane and RB5 anionic dye during the adsorption experiments.

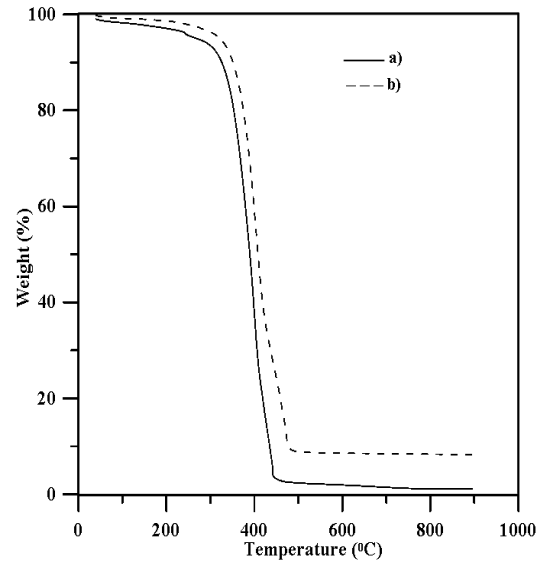


Fig. 15 TGA curves of (a) before and (b) after dye adsorption by the POM-membrane (RB5 = 15 mg/L, T = 25°C, pH = 7 at 150 rpm)

5. Conclusions

In this study, a POM-membrane was fabricated by modifying a PVDF membrane surface with poly-oxometalate ($\text{H}_5\text{PV}_2\text{Mo}_{10}\text{O}_{40}$, POM) using a chemical deposition method and characterized by FT-IR, SEM and EDX techniques, which showed that the membrane surface was modified successfully with the POM. The fabricated POM-membrane exhibited the very high RB5 dye removal efficiency (about 98% at 780 min.), but the unmodified membrane (control experiment sample) exhibited very low dye removal efficiency (about 3% at 780 min) toward the RB5 dye in the batch system. The adsorption process of the RB5 dye onto the POM-membrane showed that the adsorption of the RB5 dye increased with the increased contact time, initial dye concentration, and the adsorbent dosage. Also, as the pH value decreased, the adsorption capacity of the RB5 dye on the POM-membrane increased and the maximum adsorption capacity of the RB5 dye on the POM-membrane occurred at pH = 3 ($q_e = 29.28$ mg/g). The adsorption of the RB5 dye onto the POM-membrane showed the best fit with the Langmuir isotherm model ($q_{max} = 24.87$ mg/g, $R^2 = 0.9982$) when compared to the Freundlich, BET and Harkins-Jura isotherm models, indicating that the adsorption of RB5 dye occurred on the POM-membrane surface through monolayer adsorption. Adsorption kinetic models showed that the pseudo second order kinetic model was found the best model to fit the experimental data ($R^2 = 0.9989$, $q = 8.29$ mg/g, $C_0 = 15$ ppm). The intra-particle diffusion model showed that the intra-particle diffusion was not the only rate-limiting step. Moreover, it was found that the ratio of the adsorption capacity still remained around 93% even after four regeneration cycle, indicating that the POM-membrane contaminated with RB5 dye can be regenerable by HNO_3 acid solution and the POM-membrane can be reusable almost without loss of dye adsorption capacity. The cross-

flow membrane filtration system was conducted to perform the dye removal and separation efficiency in a single unit. Using the system, the dye removal efficiency of the POM-membrane was achieved up to 88% (at 180 min). Thus, the results show that the POM-membrane can be used as an effective adsorbent to remove the RB5 dye from the aqueous solutions.

Acknowledgements

This study is financially supported by Zonguldak Bülent Ecevit University, Research Grant No: 2017-77047330-01.

References

- Ahmad, A., Mohd-setapar, S.H., Chuong, S. and Khatoon, A. (2015), "Recent advances in new generation dye removal technologies: Novel search for approaches to reprocess wastewater", *RSC Adv.*, **5**(39), 30801-30818. <https://doi.org/10.1039/C4RA16959J>.
- Ahmed, M.J., Islam, M.A., Asif, M. and Hameed, B.H. (2017), "Human hair-derived high surface area porous carbon material for the adsorption isotherm and kinetics of tetracycline antibiotics", *Bioresour. Technol.*, **243**, 778-784. <https://doi.org/10.1016/j.biortech.2017.06.174>.
- Ai, L., Zhou, Y. and Jiang, J. (2011), "Removal of methylene blue from aqueous solution by montmorillonite/CoFe₂O₄ composite with magnetic separation performance", *Desalination*, **266**(1-3), 72-77. <https://doi.org/10.1016/j.desal.2010.08.004>.
- Ammam, M. (2013), "Polyoxometalates: Formation, structures, principal properties, main deposition methods and application in sensing", *J. Mater. Chem., A*, **1**, 6291-6312. <https://doi.org/10.1039/c3ta01663c>.
- Anbia, M., Hariri, S.A. and Ashrafizadeh, S.N. (2010), "Adsorptive removal of anionic dyes by modified nanoporous silica SBA-3", *Appl. Surf. Sci.*, **256**(10), 3228-3233. <https://doi.org/10.1016/j.apsusc.2009.12.010>.
- Arami, M., Limaee N.Y., Mahmoodi N.M. and Tabrizi N.S. (2006), "Equilibrium and kinetics studies for the adsorption of direct and acid dyes from aqueous solution by soy meal hull", *J. Hazard. Mater.*, **135**, 171-179. <https://doi.org/10.1016/j.jhazmat.2005.11.044>.
- Baral, S.S., Das, N., Roy Chaudhury, G. and Das, S.N. (2009), "A preliminary study on the adsorptive removal of Cr(VI) using seaweed, *Hydrilla verticillata*", *J. Hazard. Mater.*, **171**, 358-369. <https://doi.org/10.1016/j.jhazmat.2009.06.011>.
- Ben-Ali, S., Jaouali, I., Souissi-Najar, S. and Ouederni, A. (2017), "Characterization and adsorption capacity of raw pomegranate peel biosorbent for copper removal", *J. Clean. Prod.*, **142**, 3809-3821. <https://doi.org/10.1016/j.jclepro.2016.10.081>.
- Du, Q., Sun, J., Li, Y., Yang, X., Wang, X., Wang, Z. and Xia, L. (2014), "Highly enhanced adsorption of congo red onto graphene oxide/chitosan fibers by wet-chemical etching of silica nanoparticles", *Chem. Eng. J.*, **245**, 99-106. <https://doi.org/10.1016/j.cej.2014.02.006>.
- Ghaedi, M., Nasab, A.G., Khodadoust, S., Rajabi, M. and Azizian, S. (2014), "Application of activated carbon as adsorbents for efficient removal of methylene blue: Kinetics and equilibrium study", *J. Ind. Eng. Chem.*, **20**(4), 2317-2324. <https://doi.org/10.1016/j.jiec.2013.10.007>.
- Güzel, F., Sayılı, H., Akkaya Sayılı, G. and Koyuncu, F. (2015), "New low-cost nanoporous carbonaceous adsorbent developed from carob (*Ceratonia siliqua*) processing industry waste for the adsorption of anionic textile dye: Characterization, equilibrium and kinetic modeling", *J. Mol. Liq.*, **206**, 244-255. <https://doi.org/10.1016/j.molliq.2015.02.037>.
- Hebbar, R.S., Isloor, A.M., Inamuddin, Abdullah, M.S., Ismail, A.F. and Asiri, A.M. (2018), "Fabrication of polyetherimide nanocomposite membrane with amine functionalised halloysite nanotubes for effective removal of cationic dye effluents", *J. Taiwan Inst. Chem. Eng.*, **93**, 42-53. <https://doi.org/10.1016/j.jtice.2018.07.032>.
- Heibati, B., Rodriguez-couto, S., Amrane, A., Rafatullah, M., Hawari, A. and Al-ghouti, M.A. (2014), "Uptake of reactive black 5 by pumice and walnut activated carbon: Chemistry and adsorption mechanisms", *J. Ind. Eng. Chem.*, **20**(5), 2939-2947. <https://doi.org/10.1016/j.jiec.2013.10.063>.
- Hosseini, M., Keshtkar, A.R. and Moosavian, M.A. (2016), "Electrospun chitosan/baker's yeast nanofibre adsorbent: Preparation, characterization and application in heavy metal adsorption", *Bull. Mater. Sci.*, **39**, 1091-1100. <https://doi.org/10.1007/s12034-016-1260-5>.
- Khan, M.A., Khan, M.I. and Zafar, S. (2017), "Removal of different anionic dyes from aqueous solution by anion exchange membrane", *Membr. Water Treat.*, **3**, 259-277. <https://doi.org/10.12989/mwt.2017.8.3.259>.
- Khan, M.I., Ansari, T.M., Zafar, S., Buzdar, A.R., Khan, M.A., Mumtaz, F., Prapamonthon, P. and Akhtar, M. (2018), "Acid green-25 removal from wastewater by anion exchange membrane: Adsorption kinetic and thermodynamic studies", *Membr. Water Treat.*, **2**, 79-85. <https://doi.org/10.12989/mwt.2018.9.2.079>.
- Kumar, D. and Landry, C.C. (2007), "Immobilization of a Mo, V-polyoxometalate on cationically modified mesoporous silica: Synthesis and characterization studies", *Microporous Mesoporous Mater.*, **98**, 309-316. <https://doi.org/10.1016/j.micromeso.2006.09.023>.
- Lafi, R., Mabrouk, W. and Hafiane, A. (2019), "Removal of Methylene blue from saline solutions by adsorption and electrodialysis", *Membr. Water Treat.*, **2**, 139-148. <https://doi.org/10.12989/mwt.2019.10.2.139>.
- Laohaprapanon, S., Matahum, J., Tayo, L. and You, S.J. (2015), "Photodegradation of reactive black 5 in a ZnO/UV slurry membrane reactor", *J. Taiwan Inst. Chem. Eng.*, **49**, 136-141. <https://doi.org/10.1016/j.jtice.2014.11.017>.
- Li, F., Chen, Y., Huang, H., Cao, W. and Li, T. (2015), "Removal of rhodamine B and Cr(VI) from aqueous solutions by a polyoxometalate adsorbent", *Chem. Eng. Res. Des.*, **100**, 192-202. <https://doi.org/10.1016/j.cherd.2015.05.030>.
- Li, Q., Li, Y., Ma, X., Du, Q., Sui, K., Wang, D., Wang, C., Li, H. and Xia, Y. (2017), "Filtration and adsorption properties of porous calcium alginate membrane for methylene blue removal from water", *Chem. Eng. J.*, **316**, 623-630. <https://doi.org/10.1016/j.cej.2017.01.098>.
- Li, C., Lou, T., Yan, X., Long, Y.Z., Cui, G. and Wang, X. (2018), "Fabrication of pure chitosan nanofibrous membranes as effective adsorbent for dye removal", *Int. J. Biol. Macromol.*, **106**, 768-774. <https://doi.org/10.1016/j.ijbiomac.2017.08.072>.
- Liu, J. and Wang, X. (2013), "Novel silica-based hybrid adsorbents: Lead (II) adsorption isotherms", *Sci. World J.*, **2013**, 1-7. <http://dx.doi.org/10.1155/2013/897159>.
- Mahboub, M.N., Jafari, Z. and Khojasteh, Y. (2020), "Cost-effective polyvinylchloride-based adsorbing membrane for cationic dye removal", *Membr. Water Treat.*, **2**, 131-139. <https://doi.org/10.12989/mwt.2020.11.2.131>.
- Muller, A., Krickemeyer, E., Meyer, J., Bögge, H., Peters, F., Plass, W., Diemann, E., Dillinger, S., Nonnenbruch, F., Randerath, M. and Menke, C. (1995), "[Mo₁₅₄(NO)₁₄O₄₂₀(OH)₂₈(H₂O)₇₀](25±5): A water-soluble big wheel with more than 700 atoms and a relative molecular mass

- of about 24000", *Angew. Chem. Int. Ed.*, **34**, 2122-2124. <https://doi.org/10.1002/anie.199521221>.
- Munagapati, V.S., Yarramuthi, V., Kim, Y., Lee, K.M. and Kim, D.S. (2018), "Removal of anionic dyes (reactive black 5 and congo red) from aqueous solutions using banana peel powder as an adsorbent", *Ecotoxicol. Environ. Saf.*, **148**, 601-607. <https://doi.org/10.1016/j.ecoenv.2017.10.075>.
- Nesic, A.R., Velickovic, S.J. and Antonovic, D.G. (2012), "Characterization of chitosan/montmorillonite membranes as adsorbents for Bezactiv Orange V-3R dye", *J. Hazard. Mater.*, **209**, 256-263. <https://doi.org/10.1016/j.jhazmat.2012.01.020>.
- Özer, A. and Dursun, G. (2007), "Removal of methylene blue from aqueous solution by dehydrated wheat bran carbon", *J. Hazard. Mater.*, **146**(1-2), 262-269. <https://doi.org/10.1016/j.jhazmat.2006.12.016>.
- Patel, S. and Hota, G. (2014), "Adsorptive removal of malachite green dye by functionalized electrospun PAN nanofibers membrane", *Fibers Polym.*, **15**(11), 2272-2282. <https://doi.org/10.1007/s12221-014-2272-7>.
- Putaj, P. and Lefebvre, F. (2011), "Polyoxometalates containing late transition and noble metal atoms", *Coord. Chem. Rev.*, **255**(15-16), 1642-1685. <https://doi.org/10.1016/j.ccr.2011.01.030>.
- Rabbani, M., Seghatoleslami, Z.S. and Rahimi, R. (2017), "Selective adsorption of organic dye methylene blue by Cs₄H₂PMo₁₁FeO₄₀·6H₂O in presence of methyl orange and Rhodamine-B", *J. Mol. Struct.*, **1146**, 113-118. <https://doi.org/10.1016/j.molstruc.2017.05.134>.
- Rache, M.L., Garcia, A.R., Zea, H.R., Silva, A.M.T., Madeira, L.M. and Ramirez, J.H. (2014), "Azo-dye orange II degradation by the heterogeneous Fenton-like process using a zeolite Y-Fe catalyst-Kinetics with a model based on the Fermi's equation", *Appl. Catal. B.*, **146**, 192-200. <https://doi.org/10.1016/j.apcatb.2013.04.028>.
- Rajabi, M., Mirza, B., Mahanpoor, K., Mirjalili, M., Najafi, F., Moradi, O., Sadegh, H., Shahyari-ghoshekandi, R., Asif, M., Tyagi, I., Agarwal, S. and Gupta, V.K. (2016), "Adsorption of malachite green from aqueous solution by carboxylate group functionalized multi-walled carbon nanotubes: Determination of equilibrium and kinetics parameters", *J. Ind. Eng. Chem.*, **34**, 130-138. <https://doi.org/10.1016/j.jiec.2015.11.001>.
- Roesink, H.D.W., Beerlage, M.A.M., Potman, W., Van Den Boomgaard, T., Mulder, M.H.V. and Smolders, C.A. (1991), "Characterization of new membrane materials by means of fouling experiments Adsorption of bsa on polyetherimide-polyvinylpyrrolidone membranes", *Colloids Surf.*, **55**, 231-243. [https://doi.org/10.1016/0166-6622\(91\)80095-6](https://doi.org/10.1016/0166-6622(91)80095-6).
- Shao, L., Cheng, X.Q., Liu, Y., Quan, S., Ma, J., Zhao, S.Z. and Wang, K.Y. (2013), "Newly developed nanofiltration (NF) composite membranes by interfacial polymerization for Safranin O and Aniline blue removal", *J. Membr. Sci.*, **430**, 96-105. <https://doi.org/10.1016/j.memsci.2012.12.005>.
- Tangestaninejad, S., Moghadam, M., Mirkhani, V., Mohammadpoor-Baltork, I. and Salavati, H. (2010), "Vanadium-containing polyphosphomolybdate immobilized on TiO₂ nanoparticles: A recoverable and efficient catalyst for photochemical, sonochemical and photosonochemical degradation of dyes under irradiation of UV light", *J. Iran. Chem. Soc.*, **7**, 161-174. <https://doi.org/10.1007/bf03246195>.
- Thirumoorthy, K. and Krishna, S.K. (2020), "Removal of cationic and anionic dyes from aqueous phase by Ball clay - Manganese dioxide nanocomposites", *J. Environ. Chem. Eng.*, **8**, 103582. <https://doi.org/10.1016/j.jece.2019.103582>.
- Tsigdinos, G.A. and Hallada, C.J. (1968), "Molybdovanadophosphoric acids and their salts. I. Investigation of methods of preparation and characterization", *Inorg. Chem.*, **7**, 437-441. <https://doi.org/10.1021/ic50061a009>.
- Vakili, M., Rafatullah, M., Salamatinia, B., Abdullah, A.Z., Ibrahim, M.H., Tan, K.B., Gholami, Z. and Amouzgar, P. (2014), "Application of chitosan and its derivatives as adsorbents for dye removal from water and wastewater: A review", *Carbohydr. Polym.*, **113**, 115-130. <https://doi.org/10.1016/j.carbpol.2014.07.007>.
- Vakili, M., Rafatullah, M., Salamatinia, B., Hakimi, M. and Zuhairi, A. (2015), "Elimination of reactive blue 4 from aqueous solutions using 3-aminopropyl triethoxysilane modified chitosan beads", *Carbohydr. Polym.*, **132**, 89-96. <https://doi.org/10.1016/j.carbpol.2015.05.080>.
- Vakili, M., Rafatullah, M., Hakimi, M., Zuhairi, A., Salamatinia, B. and Gholami, Z. (2016), "Chitosan hydrogel beads impregnated with hexadecylamine for improved reactive blue 4 adsorption", *Carbohydr. Polym.*, **137**, 139-146. <http://dx.doi.org/10.1016/j.carbpol.2015.09.017>.
- Vakili, M., Rafatullah, M., Hakimi, M., Zuhairi, A., Gholami, Z. and Salamatinia, B. (2017), "Enhancing reactive blue 4 adsorption through chemical modification of chitosan with hexadecylamine and 3-aminopropyl triethoxysilane", *J. Water Process Eng.*, **15**, 49-54. <https://doi.org/10.1016/j.jwpe.2016.06.005>.
- Wang, X., Liu, Z., Ye, X., Hu, K., Zhong, H., Yu, J., Jin, M. and Guo, Z. (2014), "A facile one-step approach to functionalized graphene oxide-based hydrogels used as effective adsorbents toward anionic dyes", *Appl. Surf. Sci.*, **308**, 82-90. <https://doi.org/10.1016/j.apsusc.2014.04.103>.
- Wang, X., Li, Y., Li, H. and Yang, C. (2016), "Chitosan membrane adsorber for low concentration copper ion removal", *Carbohydr. Polym.*, **146**, 274-281. <https://doi.org/10.1016/j.carbpol.2016.03.055>.
- Weber, W.J. and Morris, J.C. (1963), "Kinetics of adsorption on carbon from solution", *Am. Soc. Civ. Eng.*, **89**, 31-60.
- Wong, S., Tumari, H.H., Ngadi, N., Mohamed, N.B., Hassan, O., Mat, R. and Saidina Amin, N.A. (2019), "Adsorption of anionic dyes on spent tea leaves modified with polyethyleneimine (PEI-STL)", *J. Clean. Prod.*, **206**, 394-406. <https://doi.org/10.1016/j.jclepro.2018.09.201>.
- Xin, S., Zeng, Z., Zhou, X., Luo, W., Shi, X., Wang, Q., Deng, H. and Du, Y. (2017), "Recyclable saccharomyces cerevisiae loaded nanofibrous mats with sandwich structure constructing via bio-electrospraying for heavy metal removal", *J. Hazard. Mater.*, **324**, 365-372. <https://doi.org/10.1016/j.jhazmat.2016.10.070>.
- Xiong, X., Jianguo, B., Hassan, O.S., Hui, G., Yu, Z. and Hong, W. (2016), "Study for adsorption behaviors of emulsion oil on a novel ZrO₂/PVDF modified membrane", *Desal. Water Treat.*, **57**, 11736-11745. <https://doi.org/10.1080/19443994.2015.1044918>.
- Yang, Y., Wang, G., Wang, B., Li, Z., Jia, X., Zhou, Q. and Zhao, Y. (2011), "Biosorption of Acid Black 172 and Congo Red from aqueous solution by nonviable Penicillium YW 01: Kinetic study, equilibrium isotherm and artificial neural network modeling", *Bioresour. Technol.*, **102**, 828-834. <https://doi.org/10.1016/j.biortech.2010.08.125>.
- Yao, L., Zhang, L.Z., Wang, R., Loh, C.H. and Dong, Z.L. (2013), "Fabrication of catalytic membrane contactors based on polyoxometalates and polyvinylidene fluoride intended for degrading phenol in wastewater under mild conditions", *Sep. Purif. Technol.*, **118**, 162-169. <https://doi.org/10.1016/j.seppur.2013.06.029>.
- Yao, L., Lua, S.K., Zhang, L., Wang, R. and Dong, Z.L. (2014), "Dye removal by surfactant encapsulated polyoxometalates", *J. Hazard. Mater.*, **280**, 428-435. <https://doi.org/10.1016/j.jhazmat.2014.08.026>.
- Yao, L., Zhang, L., Wang, R., Chou, S. and Dong, Z.L. (2016), "A new integrated approach for dye removal from wastewater by polyoxometalates functionalized membranes", *J. Hazard. Mater.*, **301**, 462-470. <https://doi.org/10.1016/j.jhazmat.2015.09.027>.

- Yıldırım, Y. and Topaloğlu, A.K. (2018), "POM based catalytic membrane contactor preparing and characterizing", *MSU J. Sci.*, **6**, 539-544. <https://doi.org/10.18586/msufbd.459266>.
- Yu, S., Liu, M., Ma, M., Qi, M., Lü, Z. and Gao, C. (2010), "Impacts of membrane properties on reactive dye removal from dye/salt mixtures by asymmetric cellulose acetate and composite polyamide nanofiltration membranes", *J. Membr. Sci.*, **350**, 83-91. <https://doi.org/10.1016/j.memsci.2009.12.014>.
- Zhang, X., Chen, M., Yu, Y., Yang, T. and Wang, J. (2011), "Polyelectrolyte-modified multi-walled carbon nanotubes for the adsorption of chromium(vi)", *Anal. Methods.*, **3**(2), 457-462. <https://doi.org/10.1039/c0ay00621a>.
- Zhang, B., Yu, S., Zhu, Y., Shen, Y., Gao, X., Shi, W. and Hwa Tay, J. (2020), "Adsorption mechanisms of crude oil onto polytetrafluoroethylene membrane: Kinetics and isotherm, and strategies for adsorption fouling control", *Sep. Purif. Technol.*, **235**, 116212. <https://doi.org/10.1016/j.seppur.2019.116212>.
- Zhao, S., Wang, X. and Huo, M. (2010), "Catalytic wet air oxidation of phenol with air and micellar molybdovanadophosphoric polyoxometalates under room condition", *Appl. Catal. B.*, **97**, 127-134. <https://doi.org/10.1016/j.apcatb.2010.03.032>.
- Zheng, H., Liu, D., Zheng, Y., Liang, S. and Liu, Z. (2009), "Sorption isotherm and kinetic modeling of aniline on Cr-bentonite", *J. Hazard. Mater.*, **167**(1-3), 141-147. <https://doi.org/10.1016/j.jhazmat.2008.12.093>.